Atmos. Chem. Phys. Discuss., 4, 2003–2036, 2004
www.atmos-chem-phys.org/acpd/4/2003/
SRef-ID: 1680-7375/acpd/2004-4-2003


Atmospheric Chemistry and Physics Discussions

# Assessment of the NO-$NO_2$-$O_3$ photostationary state applicability on long-term measurements at the GAW global station Hohenpeissenberg, Germany

**K. Mannschreck[1], S. Gilge[2], C. Plass-Duelmer[2], W. Fricke[2], and H. Berresheim[2]**

[1]Umweltforschungsstation Schneefernerhaus, Zugspitze, Germany
[2]Deutscher Wetterdienst, Meteorologisches Observatorium Hohenpeissenberg, Germany

Received: 3 February 2004 – Accepted: 3 March 2004 – Published: 7 April 2004

Correspondence to: K. Mannschreck (k.mannschreck@schneefernerhaus.de)

## Abstract

Continuous measurements of reactive gases, radiation, and meteorological parameters are carried out at the Meteorological Observatory Hohenpeissenberg (MOHp) as part of the Global Atmosphere Watch (GAW) Program. NO, $NO_2$, $O_3$ and $J_{NO_2}$ data from a four year period (March 1999–December 2002) are evaluated for consistency with photochemical steady state (PSS, $\Phi$=1) conditions. In average PSS was reached in 17%, 13%, 22% and 32% of all cases for the year 1999, 2000, 2001 and 2002, respectively. The extent of deviation from PSS reveals a strong dependence on wind direction at the station. Median values of $\Phi$ in the south sector are in the range of 2.5–5.7 and show a high variability. In contrast, values for the other directions show a relatively low variability around a median level of 2. These differences can be explained by local effects. It is shown that the height of the sample inlet line, its distance to the forest and the surrounding topography has a strong impact on both the absolute and relative deviations from PSS. Global irradiance and thus, photolysis of $NO_2$ is reduced within the dense forest. Since the reaction of NO with $O_3$ is still proceeding under these conditions, increased $NO_2$/NO ratios are produced locally in air which is transported through the forest and advected to the MOHp site.

Estimates of the peroxy radical concentration ($RO_2$) inferred from PSS are compared with peroxy radical measurements made at the site in June 2000 in a three week campaign. The PSS derived $RO_2$ levels were higher than corresponding measured levels by at least a factor of 2–3. This analysis was made for a wind sector with minimal local effects on PSS. Thus the corresponding $\Phi$ median of 2 can be regarded as an upper limit for a deviation from PSS due to chemical reactions, i.e. by peroxy radicals and possible other oxidants converting additional NO to $NO_2$.




**ACPD**

4, 2003–2036, 2004

**Assessment of the NO-$NO_2$-$O_3$ photostationary state applicability**

K. Mannschreck et al.

## 1. Introduction

NO in the troposphere is converted to $NO_2$ by reaction with $O_3$ and – during daytime – photolysed back to NO.

$$NO + O_3 \rightarrow NO_2 + O_2 \qquad k_1 = 1.4 \cdot 10^{-12} \cdot \exp(-1310/T)\,cm^3\,s^{-1} \tag{1}$$

$$NO_2 + h\nu \rightarrow NO + O(^3P) \qquad \lambda < 420\,nm \tag{2}$$

$$O(^3P) + O_2 + M \rightarrow O_3 + M. \tag{3}$$

These two processes (1)–(2) tend to establish an equilibrium on a time scale of 100 s (Leighton, 1961), known as the Photostationary State (PSS), which can be described as

$$\frac{[NO_2]}{[NO]} = \frac{k_1\,[O_3]}{J_{NO_2}} \tag{4}$$

The Photostationary State parameter Φ is defined as:

$$\Phi = \frac{J_{NO_2} \cdot [NO_2]}{k_1 [O_3][NO]}, \tag{5}$$

where $J_{NO_2}$ is the photolysis rate of $NO_2$. The value of $k_1$ in Reaction (1) is taken from Atkinson et al. (2002).

Reactions (1)–(3) determine a quasi-constant PSS ozone level which mainly depends on the $NO_2$ photolysis frequency. Mechanistically, this represents a null cycle in which no additional ozone is produced. Φ is equal to 1 when other reactions converting NO to $NO_2$ and local emissions of either compound are negligible. In particular, peroxy radicals may contribute to additional NO to $NO_2$ transformation thereby increasing ambient ozone levels beyond PSS:

$$HO_2 + NO \rightarrow NO_2 + HO \tag{6}$$



ACPD
4, 2003–2036, 2004

$$RO_2 + NO \rightarrow NO_2 + RO. \quad (7)$$

R represents any organic functional group, the simplest being $CH_3$. In the following the sum of $HO_2$ and all organic peroxy radical species is defined as $RO_2$.

At high $NO_x$ (=NO+$NO_2$) levels significant concentrations of peroxy radicals are not established due to efficient scavenging of OH – the precursor of $RO_2$ – by $NO_2$ producing $HNO_3$ and increased loss of $RO_2$ by reaction with NO. However, in low-$NO_x$ environments peroxy radicals gain importance and can perturb the PSS. In this case $\Phi$ becomes greater than unity which is often found in rural areas (e.g. Ridley, 1992; Parrish, 1986).

However, several field studies which included measurements of peroxy radicals in addition to NO, $NO_2$, $J_{NO_2}$ and $O_3$ showed that measured peroxy radical concentrations were still too low to explain the observed deviations from PSS (e.g. Cantrell et al., 1993; Davis et al., 1993; Hauglustaine et al., 1996; Volz-Thomas et al., 2003; Handisides et al., 2003). Some authors have speculated that an as yet unidentified oxidant XO might have contributed to additional conversion of NO to $NO_2$ (Parrish et al. 1986, Carpenter et al. 1998, Volz-Thomas, 2003). Assuming important contributions from both an unknown oxidant and the measured peroxy radicals, corresponding steady state conditions can be described by the extended parameter $\Phi_{ext}$:

$$\Phi_{ext} = \frac{J_{NO_2} \cdot [NO_2]}{k_1 [O_3] [NO] + k_{6-7} [RO_2] [NO] + k_{xo} [XO] [NO]}. \quad (8)$$

Further contributions to deviations from PSS may result from:

- Local $NO_2$ sources near the measurement site
- Local NO or $O_3$ sinks near the measurement site
- Other non-steady state conditions (e.g. rapid changes in $J_{NO_2}$, $O_3$...)
- Measurement errors.

Since the mid-1990's continuous long-term measurements of a broad range of important tropospheric constituents and physical parameters (e.g. $O_3$, NO, $NO_2$, $NO_y$, $J(O^1D)$, $J(NO_2)$, radiation) are conducted at the German Weather Service's (DWD) Meteorological Observatory Hohenpeissenberg (MOHp) as part of the Global Atmosphere Watch program (GAW) of the World Meteorological Organization (WMO). Measurements from March 1999 to December 2002 are evaluated in this study to examine the validity and frequency of occurrence of $O_3$/NO/$NO_2$ photostationary state. Due to construction of a new GAW building at the site during 1999 and 2000 the GAW observation platform was housed in a preliminary building during this time. This building was located relatively close to the forest. Accordingly, enhanced local influences on in situ levels of reactive compounds such as NO or $NO_2$ were to be expected, since it was assumed that the close vicinity of this building to the forest causes a heterogeneity of advected air masses. If the history of an air mass is not known, air chemical investigations can easily be misinterpreted. In order to characterise these conditions in more detail we have now evaluated these measurements with respect to PSS together with 2001–2002 measurements from the new building. The data are systematically analysed by statistical means. This includes a classification by wind direction as well as using results from previous campaign measurements of peroxy radical concentrations at MOHp (Handisides et al., 2003).

## 2. Experimental

### 2.1. Measurement site

The Meteorological Observatory Hohenpeissenberg (MOHp) of the German Weather Service is located approximately 40 km north of the Alps at 985 m a.s.l. (47°48' N, 11°01' E) at the top of a solitary hill which elevates about 300–400 m over the surrounding area. Since 1994 the station is operated (complementary with the High Alpine Environmental Research Station Schneefernerhaus) as one of the present 22 WMO Global



ACPD
4, 2003–2036, 2004

Atmosphere Watch Stations.

Generally, the site is advected by relatively clean air masses (yearly average of $NO_x$ is below 3.5 ppb), however, maximum values can sometimes reach 12–14 ppb, particularly during stagnant inversion conditions in winter when the site is within the boundary layer.

The site is surrounded by forests (70%, mostly coniferous) and agricultural pastures (30%). The distance to the nearest urban and major industrial areas (e.g. Munich) is about 80 km. In the south sector air masses are predominantly advected from the Alps region at relatively high wind speeds and trace gas concentrations in this sector are relatively low. Possible anthropogenic sources which could influence trace gas concentrations are rural road traffic and small towns (4000–12 000 inhabitants) approximately 5–8 km from the site to the south-west. Air masses from the other directions on average have lower wind speeds and show somewhat higher concentrations of trace gases. Specifically, air from north-east shows a higher level of pollution due to emissions from a small town in 10 km (20 000 inhabitants) and the city of Munich (1 Mio inhabitants) in 80 km.

During 1999 and 2000 the instruments for the trace gas measurements were operated in a preliminary building with the air inlets at approximately 10 m above ground level. This corresponded to some 2 m below the canopy tops of trees and about 3 m of horizontal distance to the nearest trees of the forest located in the sector between 105° and 290°. North of the building (290°–70°) the distance to the trees was about 100 m. To the East of the building (70°–105°) there are meadows, a parking lot and some houses but no trees.

In April 2001 the instruments were moved to the new GAW building about 100 m further north west. Sample inlets at the new location are located approx. 15 m above ground. The horizontal distance to the nearby forest in the sector between 115–135° is approx. 200 m, between 135°–190° approx. 50 m and between 190°–270° approx. 10 m. In the latter case the air inlet is approximately at the canopy height of the trees. The sector between 270°–360° is characterised by a steep slope and the inlet line is



ACPD
4, 2003–2036, 2004

well above the canopy height of the trees which are in a distance of at least 10 m in this direction. To the north east (0°–90°) the forest is about 200 m apart, however, partial shading of air parcels flowing along the north western edge of the building is possible when air is advected parallel to the ground rather than from aloft. The sector between 90°–115° is free of trees and characterised by meadows and the parking lot.

Temperature, pressure, and humidity were measured ground-based at a horizontal distance of 50 m and 100 m from the provisional and the new building, respectively, and wind measurements were made on top of a 40 m mast.

### 2.2. Measurement program

Based on Eq. (5) an experimental verification of PSS conditions requires simultaneous measurements of NO, $NO_2$, $O_3$, $J_{NO_2}$ and ambient temperature (to account for the temperature dependence of $k_1$). Table 1 summarises the analytical techniques used to determine the individual parameters.

Ozone is measured simultaneously with two UV absorption instruments (Thermo Environmental Instruments Inc., Model TECO 49C, and Dasibi), a chemiluminescence-based instrument (UPK, Germany), and a self-built wet chemical method (potassium iodide). According to GAW QA regulations, ozone analysers are calibrated in regular time intervals with a transfer standard (TECO 49 PS). In addition, ozone measurements have been validated by audits carried out by the GAW World Calibration Centre for ground-based ozone measurements (EMPA, Switzerland).

Nitrogen oxide species are measured with three analysers and two different chemiluminescence methods. Two analysers are based on chemiluminescence of NO with ozone measured with a chemiluminescence detector, CLD (ECO-Physics CLD 770 AL ppt). One of these is operated in combination with a photolytic converter, PLC (ECO-Physics PLC 760) which converts $NO_2$ to NO specifically and the other with a gold converter (gold tube at 300°C in the presence of 0.1% CO) which converts $NO_y$ to NO.

The second method makes use of the chemiluminescence of $NO_2$ reacting with luminol (Scintrex Unisearch LMA-3) which is also detected with a CLD. NO is oxidised



ACPD
4, 2003–2036, 2004

quantitatively to $NO_2$ by leading the gas flow over a $CrO_3$-filter. The luminol instrument serves as backup and for quality control. For $NO_2$ both methods agree better than 1 %.

The $NO_x$ instruments are routinely calibrated every second day with a known flow of calibration gas (5 and 10 ppm NO in $N_2$, Messer, Germany) which is dynamically diluted to atmospheric concentration ranges. The conversion efficiencies of the PLC and the gold converter for $NO_2$ are determined by measurements of $NO_2$ produced by gas phase titration of the NO standard with ozone. In addition, the $NO_y$ measurements are checked with a $HNO_3$ permeation source (self-built). Deviations between two calibrations are typically well below 2%.

For quality control several informal intercomparisons with other instruments under calibration and ambient air conditions were carried out in the last years, the last one in August 2002. Under ambient air conditions (ranges: lower than detection limit up to 1.3 ppb for NO, 0.4–4.3 ppb for $NO_2$, 2.3–4.5 ppb for $NO_y$) the deviations between the two systems (MOHp and German Aerospace Centre, DLR Oberpfaffenhofen) were well below 5% in the case of NO, below 1% for $NO_2$ and below 5% for $NO_y$ at correlation coefficients of r=0.96, 0.98 and 0.90, respectively. Thus, the deviations are smaller than the overall measurement uncertainties (MOHp/DLR) of 5.3%/5.9%, 5.7%/7.5% and 10.3%/8.6% for NO, $NO_2$ and $NO_y$, respectively.

$J_{NO_2}$ is quantified by measuring the UV actinic flux with two (up- and downward) $2\pi$ steradian filter radiometers. The radiometers are calibrated by two different references: In 1997, the filter radiometers were calibrated against a “master” filter radiometer by the manufacturer. This master filter radiometer had been calibrated by a chemical actinometer in 1996, which had an accuracy of about 8%. In 2001 the filter radiometers were again calibrated by the master filter radiometer, the sensitivity had changed in the corresponding period of 4 years by less than 3%. Later in 2001, the filter radiometers were calibrated versus an actinic spectral radiometer by Research Centre Jülich, which had been compared with chemical actinometry (Kraus et al., 2000). This resulted in an accuracy of our filter radiometers of 13% each, based on the accuracy of the spectral



ACPD
4, 2003–2036, 2004

radiometer for measurement of $J_{NO_2}$ of 10% (Kraus et al., 2000). The calibration results in comparison to the spectral radiometer differed by 7% from the calibration with respect to the master filter radiometer in 2001, which is consistent within the range of the specified accuracy. For calculation of $J_{NO_2}$ from spectral radiometer data, the $NO_2$ absorption cross section determined by Merienne et al. (1995) and the quantum yields determined by Troe (2000) were used. For the period 1999 to 2001, the filter radiometer results obtained for clear sky conditions were checked for sensitivity changes by comparison with $J_{NO_2}$ values calculated by the model STAR (System for Transfer of Atmospheric Radiation, Schwander et al., 2001). The radiometer sensitivities showed small changes by less than 2% from year to year, which is not significant. Following the calibration in Jülich, the filter radiometers were regularly checked by measurement of their sensitivity using an optical bench setup with 2 different 1000 W quartz halogen reference lamps. In the years 2001 to 2003 the sensitivity showed insignificant changes of less than 1.5% from year to year. Thus, our $J_{NO_2}$ data for 1999–2002 at levels above $6{\cdot}10^3\,s^1$ had an overall accuracy of 14% and a precision of better than 2%.

### 2.3. Data base

One minute time-resolved data obtained for all meteorological, physical and chemical parameters were averaged to 10 min mean values. Each year of the total period under investigation (March 1999–December 2002) is separately analysed.

Only very sunny periods (filtered by the condition $J_{NO_2} \geq 6{\cdot}10^{-3}\,s^{-1}$) were selected to verify photostationary state conditions. Based on 10 min mean $NO_x$ values Table 2 shows the total number of all data available from the above period, the number of all data with $J_{NO_2} \geq 6{\cdot}10^{-3}\,s^{-1}$, and the number of available $\Phi$ values, which could be derived from simultaneous measurements of $NO_2$, NO, $O_3$, $J_{NO_2}$ and T and discriminated by $J_{NO_2} \geq 6{\cdot}10^{-3}\,s^{-1}$. Figure 1 presents the frequency distribution of the wind direction averaged over the 4 year period. In general, the prevailing wind direction at MOHp is WSW followed by NE. When applying the criterion for $J_{NO_2}$, the relative amount of data

is significantly reduced for the WSW sector and increased for the NE sector so that the relative frequency becomes similar for both sectors.

## 3. Experimental results

Figure 2 presents the dependence of the mean annual CO and $NO_x$ concentrations on wind direction for daytime clear sky conditions ($J_{NO_2} \geq 6 \cdot 10^{-3}$ $s^{-1}$) for each year. CO and $NO_x$ are tracers for anthropogenic pollution mainly originating from road traffic, industrial and domestic combustion processes. The typical atmospheric lifetimes of $NO_x$ and CO with respect to reaction with OH are less than 1 day and 3–4 weeks, respectively. CO has a uniform distribution for all directions with a slight enhancement in the sector 0–100°. $NO_x$ levels are more variable with a minimum in the sector 300°–40°. Note that without $J_{NO_2}$ filtering (i.e. using all available data) the corresponding wind directional plots for $NO_x$ look somewhat different showing a $NO_x$ maximum in the NE direction due to emissions from the urban region of Munich (80 km distance). In this sector the percentage of clear sky data is above average (see Fig. 1). Since the lifetime of $NO_x$ is reduced during periods of high $J_{NO_2}$, the mean $NO_x$ values are lowered disproportionally when applying the $J_{NO_2}$ filter criterion. The maxima observed for the clear sky data originate from small towns in a distance of about 10 km.

The dependence of the median values of $\Phi$ on wind direction is shown in Fig. 3. $\Phi$ was determined as defined in Eq. (5). While during all years $\Phi$ is around 2 for the west, north and east sector, the two periods 1999–2000 (preliminary building) and 2001–2002 (new building) show differences in the south sector. During 1999–2000 $\Phi$ medians of 3.5–5.7 are found for the sector 130°–260°, and values of 2.5–3.8 for the sector 150°–250° during 2001–2002.

In Fig. 4 the frequency distribution of cases in which PSS conditions prevailed is presented. Here, $\Phi_{ext}$ is shown calculated using Eq. (8) with [XO]=0 and taking into



ACPD
4, 2003–2036, 2004

account a $RO_2$ mixing ratio which was determined as a function of $J_{NO_2}$[1]. All data with $\Phi_{ext}=1\pm0.2$ are included in the distribution.

During 1999 and 2000 PSS was reached in 17% and 13% of all cases, respectively. While the highest percentage (approx. 40%) is reached for the east sector (80°–100°), PSS is reached in less than 20% of cases for all other wind directions. During 2001 and 2002 PSS was reached in 22% and 32% of all cases, respectively with a maximum of approx. 60% for NW.

## 4. Discussion

Our results show that deviations from PSS at MOHp are influenced most by the history of an air parcel which is associated with the wind directions. A secondary but still significant contribution is due to the characteristic differences between the two measurement sites as described earlier.

Published studies based on similar measurement conditions (rural or suburban) report Φ values of 1–3 (Parrish, 1986; Hauglustaine et al., 1996; Volz-Thomas et al., 2003) and 1.8–1.9 (Rohrer, 1998; Ridley et al., 1992). Our results are similar to these data except for the sector 130°–260° during 1999–2000 which exhibits values higher by a factor of 2.

Several previously conducted experiments also included measurements of peroxy radicals which were then compared with PSS theory. These studies included measurements under different levels of pollution: $[NO_x]<0.1$ ppb (Hauglustine, 1996), $NO_x$ 0.1–1.5 ppb (Cantrell, 1993; Davis, 1993; Frost, 1998; Cantrell 1997) and $NO_x>1.5$ ppb (Volz-Thomas, 2003; Baumann, 2000; Carpenter, 1998). Generally, $RO_2$ concentrations calculated from assuming PSS were significantly higher than directly measured

[1]Based on the measurements of $RO_2$ during a 3 week campaign at MOHp (see next section), the dependence of $[RO_2]$ on $J_{NO_2}$ can be described as a first approximation using the following linear equation: $[RO_2] = 3214*J_{NO_2}\ [s^{-1}] + 13$ (in units of ppt).



ACPD
4, 2003–2036, 2004

values. $NO_x$ levels at MOHp are typically in the range of 0.5–3 ppb but can reach higher values especially in winter due to frequently enhanced emissions and sustained inversion layers reaching up to the site. Possible causes which could explain the deviations from PSS observed at MOHp including their differences between individual wind sectors are discussed in the following section.

The overall uncertainty of Φ can be calculated by propagation of errors using the individual uncertainty in each parameter (given in Table 1) from Eq. (9).

$$\sigma_{\Phi} = \sqrt{\sum \left(\sigma_{Y_i}\right)^2 \cdot \left(\frac{\delta \Phi}{\delta Y_i}\right)^2}. \quad (9)$$

Generally, for $NO_x$>1 ppb the overall uncertainty is 20% on average and is dominated by the uncertainty of $J_{NO_2}$. For smaller $NO_x$ mixing ratios the uncertainty resulting from the measurement of NO dominates the overall uncertainty which approaches 60% with decreasing $NO_x$. Using Eq. (9) we have not considered the uncertainty of 5% in both NO and $NO_2$ arising from the uncertainty in the NO calibration gas as a systematic error which does not contribute to the uncertainty of the ratio.

The differences in Φ values observed between the two periods for each wind sector (Fig. 3) are not significant on a 1$\sigma$ confidence level. Differences between the sector 130°–260° and the remaining wind directions for 1999–2000 are significant on a 1$\sigma$ confidence level, differences between the sector 150°–250° and the remaining wind directions for 2001–2002 are not significant. However, note that all results are based on one data series (i.e. same instrument, same calibration procedures etc.). Therefore, we may assume that measurement errors for one wind direction generally do not have the opposite sign as for the other. Furthermore, in the case of $J_{NO_2}$ the uncertainty is dominated by systematic uncertainties due to actinometry or the assumed absorption cross section and quantum yields. As stated earlier (Sect. 2.2.), the precision of $J_{NO_2}$, a measure which is more meaningful when comparing the two data sets, is better than 2%.

In order to investigate the reasons for the observed differences between the wind

directions two sectors are defined according to their level of deviation from PSS: Sector A (small deviation from PSS): 290°–110°; sector B (large deviation from PSS): 150°–260°. These two sectors are chosen as intersections of both periods so that they can be applied for both periods under investigation. Figure 5 compares the $NO_2$/NO ratios as a function of NO for sectors A and B for 1999 as an example.

In our data the dependence of $NO_2$/NO on NO corresponds to the dependence of Φ on NO. This variation is in accordance with the current understanding of radical photochemistry (see Eqs. 6 and 7). For high $NO_x$ concentrations the levels of peroxy radicals should approach zero, since the sink for $RO_2$ increases with increasing NO and since OH as a precursor for $RO_2$ as well as RO species are removed via reaction with $NO_2$.

For both sectors the variability of $NO_2$/NO ratios increases with decreasing NO mixing ratios. Generally, high scattering at low NO levels is expected, since the uncertainty in NO measurements close to the detection limit becomes relatively high. For example, when assuming an uncertainty of 50% at 30 ppt NO and $NO_2$/NO = 20, a scatter of ±50% (i.e. $NO_2$/NO=10–30), as observed for sector B, could be explained by the uncertainty in NO measurements alone. However, this strong variability is not observed for sector A. This indicates firstly, that the uncertainty is somewhat overestimated and secondly, that the strong scatter for sector B at low NO concentrations is at least partly due to the fact that the PSS equilibrium in these cases was not fully established resulting in higher values of $NO_2$/NO. Here we hypothesise that this deviation from PSS mainly resulted from the fact that the transport time from the point of PSS disturbance (e.g. by a local source of $NO_2$, or sink of $O_3$ or NO) to the measurement site was too short to re-establish PSS and/or the $NO_2$ photolysis over a large area in this sector did not vary as suggested by the $J_{NO_2}$ values measured at the MOHp site.

During 1999 and 2000 the mean $NO_2$ fraction of $NO_x$ for WSW and NE was 90% and 85%, respectively. A $NO_2$ source which could disturb the PSS leading to higher values and a high variability must therefore produce a local $NO_2$ fraction in this range. Possible local $NO_2$ sources are diesel vehicles. However, maximum $NO_2$ fractions

found in $NO_x$ emissions from diesel engines never exceeded 60–80%. Moreover, the traffic density is very low in the vicinity of the site except for occasional tourist traffic about 300 m to the east, and in WSW direction the distance to the only country road is at least 700 m. Hence, we conclude that diesel vehicles have not been the major cause for the observed deviations from PSS.

On the other hand, a possible sink for ozone is dry deposition, e.g. within the forest. Due to the close vicinity to the forest and the steep slope in southerly direction of the preliminary building air masses advected from this sector are more likely to be transported through the forest than air masses from other directions. If depositional loss of ozone is significant during transport through the forest this would lead to increased $\Phi$ values for the south sector. The significance of this potential PSS deviation was investigated by comparing the ozone measurements taken from the provisional building with those measured simultaneously on top of a nearby tower (height of inlet line: 50 m above ground, 30 m above canopy height) during 1999 and 2000. It is assumed that air masses reaching the top of the tower have been – to a higher percentage – transported above the forest canopy rather than being "filtered" through the forest in contrast to air masses reaching the lower sampling point of the provisional building. The comparison between both measurement positions showed no differences in ozone levels within the measurement uncertainty. This shows that dry deposition of ozone was not large enough to explain any of the observed differences in $\Phi$.

A possible explanation for the observed scattering in the $NO_2$/NO ratio for sector B would be a source of $NO_x$ with a variable emission flux and close distance to the measurement site so that time is too short for PSS to be established. Figure 6 shows the dependence of $NO_x$ on wind direction on the basis of 5, 10, 20, 50, 80, 90 and 95 percentiles for the year 2000 as an example. A variable source should show a distribution which is broader in the respective sector. However, this is not the case, no such signal can be detected.

Figure 7 shows that not only the median values of $\Phi$ are relatively higher in wind sector B but that also the differences between the various percentiles are larger (note

the logarithmic scale). Only the plots for 2000 and 2002 are shown as examples. For 2000 the 5 and 95 percentiles for sector B are −52% and +107% of the median, respectively and −40% and +63% of the median for sector A. For 2002 the variation is −47% and +121% for sector B and −34% and +58% for sector A.

The strong dependence of the $NO_2$/NO ratio, the Φ value and the variation of Φ on the wind direction, as well as the fact that similar results are found for the two periods respectively, i.e. preliminary building and new building, indicates that local effect at the sites have a great influence on the establishment of PSS. Apart from the height of the inlet line, the two sites differ in their direct surrounding in terms of topography and natural cover. As described in Sect. 2.1, in the case of the preliminary building, the forest extends from east to west in southerly direction with some single trees being as close as 3 m away from the building. To the west, free advection of air is obstructed by a second nearby building. Therefore, advection of air masses from the east is relatively unobstructed compared to southerly and westerly direction.

In the case of the new building the WNW sector is characterised by a steep inclination and the forest in this direction is less dense than in the other directions (e.g. WSW). Advection of air from S, SW and NE is hindered by the building itself and air is likely to encounter shaded areas under the trees and the building before reaching the sample inlet. Free advection of air masses from NW direction should therefore be favoured compared to the other directions.

### 4.1. Synthesis of data interpretation

Our explanation for the observed influence of the station's surrounding on PSS is as follows: $NO_2$/NO ratios of air masses which are transported from within the forest will increase within the forest (1 km pathway) due to reaction of NO with $O_3$. At the same time, the major source of NO, namely photolysis of $NO_2$, is substantially reduced due to reduced light penetration within the denser forest area. For an air parcel arriving from the forest the time is too short (less than 2 s for the mean wind speed of 6 m/s) to establish steady state conditions before being analysed. The measured air is most likely a

mixture of air parcels from within the forest and aloft, the share being dependent on the surrounding orography, boundary layer structure and thermal convection. On the other hand free advection enables photolysis of $NO_2$ leading to a higher percentage of PSS cases. It can be concluded that local factors such as vegetation, topography, relative position of the inlet line and advection patterns of air masses have a great influence on PSS and could obscure chemical mechanisms. Similar factors may have influenced previous campaign studies in various environments and should be considered in future field experiments. This result of the present study is of general importance and not restricted to the specific environment of MOHp.

The reason for the extremely low frequency of PSS conditions in the northern direction for the preliminary building and north easterly direction for the new building is not yet clear at this time, since for both sites the forest in this direction is not closer than to the east. However, it is assumed that the topography – namely the relatively smooth slope to the north and north east - influences the wind flow streamlines leading to a higher percentage of air flow through and thus, a longer residence time in the forest.

From 18 June until 6 July 2000, measurements of $RO_2$ using a chemical amplifier technique were performed at the site (Handisides, 2003). Daytime maximum $RO_2$ levels were 50–70 ppt for clear sky conditions, the accuracy was better than 60%. The results from these measurements are used here to investigate how large deviations from PSS are under conditions with minimum interference by local effects. As taken from Fig. 7 sector 0°–80° exhibits the smallest median values of Φ and the lowest variation in Φ during 2000. According to the earlier discussion it is assumed that for this sector potential impacts on PSS from forest "filtration" were minimal. Therefore, data from this sector are used to compare measured and PSS derived peroxy radical mixing ratios. PSS derived $RO_2$ levels were determined from

$$RO_2 = \frac{J_{NO_2} \cdot [NO_2] - [O_3] \cdot [NO] \cdot k_1}{[NO] \cdot k_{6-7}}. \quad (10)$$

$k_{6-7}$ is the average rate coefficient for the reaction of the different peroxy radicals with

NO. Handisides et al. (2003) assumed that 50% of $RO_2$ radicals are $HO_2$ and the main part of organic peroxy radicals is $CH_3O_2$. Therefore, $k_{6-7}$ was calculated as the average of the rate coefficients of reactions with $HO_2$ and $CH_3O_2$ as given by Atkinson et al. (2002). The assumptions concerning the partitioning of $RO_2$ were discussed by Handisides et al. (2003). It was found that the average rate constant is only weakly sensitive towards assuming other partitionings. For example, assuming a 2:1 ratio between the levels of organic peroxides and $HO_2$, and assuming that 50% of the organic peroxides are organics with longer R chains than methyl, the average rate constant would still only change by a few percent.

The overall diurnal $RO_2$ variation measured during this period is shown in Fig. 8. The error bars refer to the $1\sigma$ standard deviation of the 10 min mean values. Clearly, PSS derived $RO_2$ values are systematically higher than measured $RO_2$ values by a factor of 2–3. They also show a higher variability. The uncertainty in PSS derived $RO_2$ concentrations is high since they are calculated from the difference between two terms of similar magnitude. When using the PSS derived $NO_2$/NO ratio with directly measured $NO_2$/NO ratios for comparison the uncertainty is reduced (Cantrell et al., 1997). Rearranging Eq. (10) to solve for $NO_2$/NO yields:

$$\frac{[NO_2]}{[NO]} = \frac{1}{J_{NO_2}} \left( k_{6-7} \cdot [RO_2] + k_1 \cdot [O_3] \right). \quad (11)$$

The uncertainties for the measured and PSS derived $NO_2$/NO ratios were calculated by propagation of errors. Average uncertainties of 17% for measured and 20% for PSS derived $NO_2$/NO ratios were determined.

The deviations of PSS derived $NO_2$/NO ratios from measured ratios are plotted in Fig. 9 against NO. The dotted line refers to the mean uncertainty of the parameter calculated for NO classes of 0.02 ppb intervals from the square root of the sum of uncertainties of measured and PSS derived ratios. Only 35% of all data points lie within this uncertainty range. For 62% of the data points the deviation is higher, so it can not be explained by statistical errors. For the remaining 5 data points the PSS derived $NO_2$/NO ratio is higher than the measured one.



ACPD
4, 2003–2036, 2004

Using the $k_1$ value recommended by the NASA panel ($3.0 \cdot 10^{-12} \cdot \exp(-1500/T)$, Sander et al., 2003) yields a slightly better agreement between measured and PSS derived data compared with the Atkinson et al. (2002) value. The mean deviation as calculated for Fig. 8 is reduced from 27% to 23%.

As discussed above local effects should be small for the selected wind sector and therefore, the corresponding Φ median value of 2 can be regarded as an upper limit for a deviation from PSS due to chemical factors. Since the measured $RO_2$ levels are too low by a factor of 2–3 to explain this deviation, it is concluded that unknown oxidation processes must be important.

Major contributions from halogen or halogen oxide radicals which could efficiently convert NO to $NO_2$ are not likely since mixing ratios would have to be in the 30 ppt range to explain the observed deviations from PSS in conjunction with the measured $RO_2$. However, concentrations over 5 ppt are unlikely to occur in rural continental air (Hausmann and Platt, 1994). If there is an unknown oxidant which causes the deviations, it is difficult to characterise its nature and to assess its importance without direct measurements. Correlations of Φ with other species which are measured on a routine basis at MOHp ($SO_2$, ROOH, number of particles, surface of particles) did not show any relation which could explain this phenomenon. Volz-Thomas et al. (2003) addressed the question if an unknown oxidation process may lead to a net production of ozone or, alternatively, if an unknown species X is formed with simultaneous consumption of ozone. From ozone budget calculations for a city plume based on airborne measurements at different points of the plume the authors concluded that the unknown process does not lead to a net ozone production.

Beside the possibility of an unknown oxidant other factors have been discussed in literature and should be taken into consideration.

Calvert and Stockwell (1983) found that at low $NO_x$/CO and $NO_x$/hydrocarbon ratios (<0.05 and 0.2, respectively) artefact deviations from PSS due to rapid changes in $O_3$ concentration are significant. These changes can be caused by reactions other than photochemical production of ozone. Carpenter et al. (1998) discuss the loss reaction

of ozone with $HO_2$ radicals which competes with the reaction of $O_3$ and NO under clean tropospheric conditions ([NO]<50 ppt). The strong increase in $NO_2$/NO (and Φ) with decreasing NO at low NO levels which is observed in our data (Fig. 5) could be explained by such processes. The ozone mixing ratios in all our data are highest at low $NO_x$ levels and the $NO_x$/CO ratio is lower than 0.05 for more than 99% of all data. However, rapid changes in ozone concentrations are not observed. The question remains open to which extent these processes contribute to the observed deviations.

The use of Eq. (10) to calculate peroxy radicals implies that steady state conditions are reached and maintained at all times. However, it is possible that rapid changes of the solar flux by rapidly changing cloud cover causes some scatter or even a bias in the results of the PSS method. This question was investigated by Cantrell et al. (1993) in model calculations simulating changes in solar flux observed during the ROSE field experiment. These theoretically determined $RO_2$ values showed strong spikes as the solar flux increased (positive) and decreased (negative) and agreed well with PSS derived values when the solar irradiance was relatively constant for several minutes. It could be concluded from these results that variations in the solar irradiance as encountered during ROSE can introduce significant scatter in the PSS data and provide a bias towards higher PSS derived $RO_2$ levels. To test this effect in the MOHp data set presented here, the data were selected to include only data for which the $J_{NO_2}$ values before and after a $RO_2$ measurement was higher than 0.006 $s^{-1}$. Since the situation of intermittent attenuation of the sunlight by clouds is not typical for MOHp the data selection only affects 3% of the data points. Artefact deviation due to rapid changes in the solar flux can thus be excluded for the MOHp data.

## 5. Conclusions

Continuous long-term measurements of NO, $NO_2$, $O_3$, $J_{NO_2}$ of a four year period were used to investigate photostationary state (PSS) conditions at the MOHp site and to reveal conditions which lead to deviations from PSS. The pollution level of advected air

masses is relatively low (yearly average of $NO_x$ is below 3.5 ppb), however, maximum values can sometimes reach more than 10 ppb. In average PSS (i.e. $\Phi_{ext}=1\pm0.2$) was reached in 17% (1999), 13% (2000), 22% (2001) and 32% (2002) of all cases with a strong dependence on wind direction.

A discussion of these results indicates that local conditions cause the main part of the deviations. It could be shown that $\Phi$ is strongly dependent on the height of the sampling point relative to the nearby vegetation, the horizontal distance to the forest, and the general orography determining the air flow to the station. We conclude that photolysis of $NO_2$ is reduced with the reduction of light penetration in the forest sub-canopy leading to increased $NO_2$/NO ratios due to reaction of NO with $O_3$ in air masses which are transported through the forest. These effects can be large enough to obscure chemical reactions, e.g. involving an unknown oxidant.

In order to analyse factors other than the local effects, PSS derived and $RO_2$ radicals measured during a campaign are compared for a sector for which local effects are found to be smallest. PSS derived $RO_2$ were systematically higher than measured ones by a factor of 2–3. Thus, other oxidation processes must be assumed to explain the observed discrepancy.

The identification of the local effect and its influence on the deviation from PSS was only possible because a relatively large data base was available from continuous long-term measurements at the site. Data from a short-term campaign could not have revealed the effects. The conditions at MOHp in terms of location and surrounding are, however, not unusual for ground stations. Other stations at which deviations from PSS are observed may have been influenced by local effects to a similar degree.

*Acknowledgement.* The authors would like to thank R. T. Wilhelm, R. Schafranek and E. Tensing for their technical assistance. The help of B. Bohn and A. Hofzumahaus (FZ-Jülich, Germany) with calibrating our filter radiometers and discussing the accuracy of $J_{NO_2}$ measurements is gratefully acknowledged.

## References


Atkinson, R., Baulch, D. L., Cox, R. A., Crowley, J. N., Hampson Jr., R. F., Kerr, J. A., Rossi, M. J., and Troe, J.: Summary of Evaluated Kinetic and Photochemical Data for Atmospheric Chemistry, IUPAC Subcommitee on Gas Kinetic Data Evaluation for Atmospheric Chemistry, Web Version 2002.

Baumann, K., Williams, E. J., Angevine, W. M., Roberts, J. M., Norton, R. B., Frost, G. J., Fehsenfeld, F. C, Springston, S. R., Bertman, S. B., and Hartsell, B.: Ozone production and transport near Nashville, Tennessee: Results from the 1994 study at New Hendersonville, J. Geophys. Res., 105, D7, 9137–9153, 2000.

Calvert, J. G. and Stockwell, W. R.: Deviations from the $O_3$-NO-$NO_2$ photostationary state in tropospheric chemistry, Can. J. Chem., 61, 983–992, 1983.

Cantrell, C. A., Shetter, R. E., Calvert, J. G., Parrish, D. D., Fehsenfeld, F. C., Goldan, P. D., Kuster, W., Williams, E. J., Westberg, H. H., Allwine, G., and Martin, R.: Peroxy Radicals as measured in ROSE and estimated from Photostationary State Deviations, J. of Geophys. Res., 98, D10, 18 355–18 366, 1993.

Cantrell, C. A., Shetter, R. E., Calvert, J. G., Eisele, F. L., Williams, E., Baumann, K., Brune, W. H., Stevens, P. S., and Mather, J. H.: Peroxy radicals from photostationary state deviations and steady state calculations during the Tropospheric OH Photochemistry Experiment at Idaho Hill, Colorado, 1993, J. Geophys. Res., 102, D5, 6369–6378, 1997.

Carpenter, L. J., Clemitshaw, K. C., Burgess, R. A., Penkett, S. A., Cape, J. N., and McFaden, G. G.: Investigation and evaluation of the $NO_x/O_3$ Photochemical Steady State, Atmos. Environ. 32, 19, 3353–3365, 1998.

Davis, D. D., Chen, G., Chameides, W., Bradshaw, J., Sandholm, S., Rodgers, M., Schendal, J., Madronich, S., Sachse, G., Gregory, G., Anderson, B., Barrick, J., Shipham, M., Collins, J., Wade, L., and Blake, D.: A Photostationary State Analysis of the $NO_2$-NO System Based on Airborne Observations From the Subtropical/Tropical North and South Atlantic, J. Geophys. Res., 98, D12, 23 501–23 523, 1993.

Frost, G. J., Trainer, M., Allwine, G., Buhr, M. P., Calvert, J. G., Cantrell, C. A., Fehsenfeld, F. C., Goldan, P. D., Herwehe, J., Hübler, G., Kuster, W. C, Martin, R., McMillen, R. T., Montzka, S. A., Northon, R. B., Parrish, D. D., Ridley, B. A., Shetter, R. E., Walega, J. G., Watkins, B. A., Westberg, H. H., and Williams, E. J.: Photchemical ozone production in the rural southeastern United States during the 1990 Rural Oxidants in the Southern Environment

(ROSE) program, J. Geophys. Res., 104, D17, 22 491–22 508, 1998.
Handisides, G. M., Plass-Dülmer, C., Gilge, S., Bingemer, H., and Berresheim, H.: Hohenpeissenberg Photochemical Experiment (HOPE 2000): Measurements and photostationary state calculations of OH and peroxy radicals, Atmos. Chem. Phys., 3, 1565–1588, 2003.
Hauglustaine, D. A., Madronich, S., Ridley, B. A., Walega, J. G., Cantrell, C. A., and Shetter, R. E.: Observed and model-calculated photostationary state at Mouna Loa Observatory during MLOPEX 2, J. Geophys. Res., 101, D9, 14 681–14 696, 1996.
Hausmann, M. and Platt, U.: Spectroscopic measurement of bromine oxide and ozone in the high Arctic during Polar Sunrise Experiment 1992, J. Geophys. Res., 99, 25 399–25 413, 1994.
Kraus, A., Rohrer, F., and Hofzumahaus, A.: Intercomparison of $NO_2$ photolysis frequency measurements by actinic flux spectroradiometry and chemical actinometry during JCOM97, J. Geophys. Res., 27, 1115–1118, 2000.
Leighton, P. A.: Photochemistry of Air Pollution, Academic, San Diego, California, 1961.
Merienne, M. F., Jenouvrier, A., and Coquart, B.: The $NO_2$ absorption spectrum: 1. Absorption cross sections at ambient temperature in the 300–500 nm region, J. Atmos. Chem., 20, 281–297, 1995.
Parrish, D. D., Trainer, M., Williams, E. J., Fahey, D. W., Hübler, G., Eubank, C. S., Liu, S. C., Murphy, P. C., Albritton, D. L., and Fehsenfeld, F. C.: Measurements of the $NO_x$-$O_3$ Photostationary State at Niwot Ridge, Colerado, J. Geophys. Res., 91, D5, 5361–5370, 1986.
Ridley, B. A., Madronich, S., Chatfiled, R. B., Walega, J. G., Shetter, R. E., Carroll, M. A., and Montzka, D. D.: Measurements and Model Simulations of the Photostationary State during the Mauna Loa Observatory Photochemistry Experiment: Implications for Radical Concentrations and Ozone Production and Loss Rates, J. Geophys. Res., 97, D7, 10 375–10 388, 1992.
Rohrer, F., Brüning, E. S., Grobler, E. S., Weber, M., Ehhalt, D. H., Neubert, R., Schüßler, W., and Levin, I.: Mixing Ratios and Photostationary State of NO and $NO_2$ observed during the POPCORN Field Campaign at a Rural Site in Germany, J. Atmos. Chem., 31, 119–137, 1998.
Sander, S. P., Friedl, R. R., Golden, D. M., Kurylo, M. J., Huie, R. E., Orkin, V. L., Moortgat, G. K., Ravishankara, A. R., Kolb, C. E., Molina, M. J., and Finlayson-Pitts, B. J.: Chemical Kinetics and Photochemical Data for Use in Atmospheric Studies, http://jpldataeval.jpl.nasa.



ACPD
4, 2003–2036, 2004

gov/, 2003.
Schwander, H., Koepke, P., Ruggaber, A., Nakajima, T., Kaifel, A., and Oppenrieder, A.: STARSci 2.1: System for Transfer of Atmospheric Radiation, http://www.meteo.physik.uni-muenchen.de/strahlung/uvrad/Star/STARinfo.htm, 2001.
Troe, J.: Are primary quantum yields of $NO_2$ photolysis at $\lambda \leq 398$ nm smaller than unity? Zeit. Phys. Chem., 214, 5, 573–581, 2000.
Volz-Thomas, A., Pätz, H. W., Houben, N., Konrad, S., Mihelcic, D., Klüpfel, T., and Perner, D.: Inorganic trace gases and peroxy radicals during BERLIOZ at Pabstthum: An investigation of the photo stationary state of $NO_x$ and $O_3$, J. Geophys. Res., 108, D4 10.1029/2001JD001255, 2003.

**Table 1.** Analytical techniques employed at MOHp. Uncertainty and detection limit refer to a time interval of 10 min.

| Parameter | Instrument | Uncertainty ($\pm 1\sigma$) | Detection limit |
|---|---|---|---|
| NO | CLD 770AL (EcoPhysics) | 5.3% (min. 15 ppt) | 15 ppt |
| $NO_2$ | CLD 770AL (EcoPhysics)<br>Photolytic converter<br>(PLC, EcoPhysics)<br>Luminox LMA-3 | 5.7% (min. 30 ppt) | 20 ppt |
| | Scintrex Unisearch S.A. | 8% (min. 50 ppt) | 50 ppt |
| $NO_y$ | CLD 770AL (EcoPhysics)<br>Gold converter | 10.3% (min. 50 ppt) | 50 ppt |
| $O_3$ | TECO 49C (Thermo Env. Instr.) | 4.5% | 1 ppb |
| $J_{NO_2}$ | Filterradiometer, Meteorologie<br>Consult GmbH, Germany | 14% | $<1 \cdot 10^{-5}\ s^{-1}$ |



ACPD
4, 2003–2036, 2004

**Table 2.** Number of 10 min mean values for each year. Second column refers to the number of all $NO_x$ values, third column to all $NO_x$ values for which $J_{NO_2} \geq 6 \cdot 10^{-3}\ s^{-1}$, and last column to number of data for which Φ values were calculated, i.e. simultaneous measurements of $NO_2$, NO, $O_3$, $J_{NO_2}$ and T were available and $J_{NO_2} \geq 6 \cdot 10^{-3}\ s^{-1}$.

| Year | Number of all data | Number of data with $J_{NO_2} \geq 6 \cdot 10^{-3}\ s^{-1}$ | Number of Φ values |
|---|---|---|---|
| 1999 | 36 408 | 6200 | 4467 |
| 2000 | 46 434 | 6144 | 5376 |
| 2001 | 46 447 | 5431 | 4970 |
| 2002 | 48 313 | 6973 | 6778 |



ACPD
4, 2003–2036, 2004

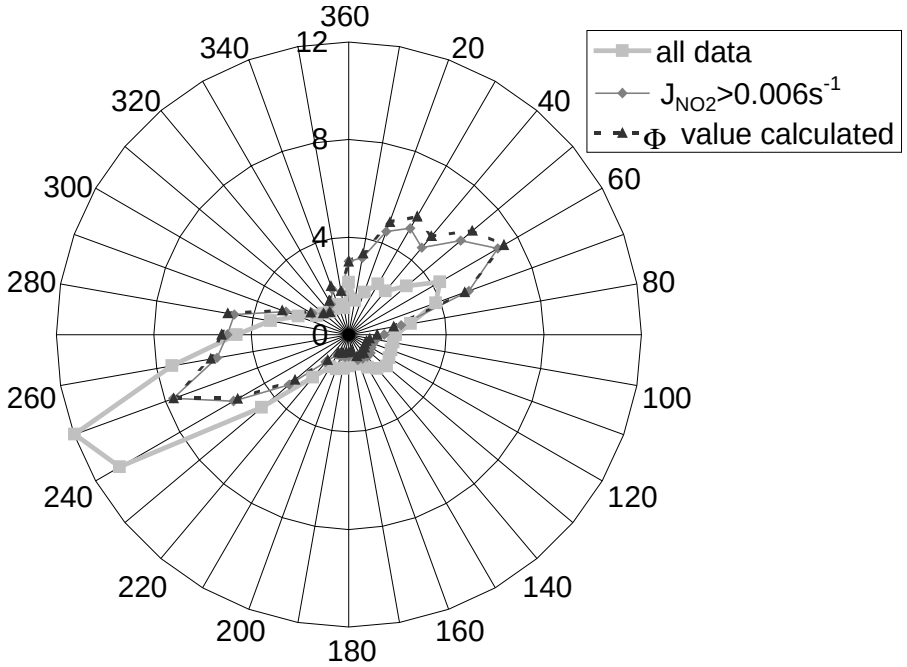


**Fig. 1.** Average relative frequency of wind direction in % for the period March 1999–December 2002. Bold grey line: all data, thin grey line: all data for which $J_{NO_2} \geq 6 \cdot 10^{-3}\,s^{-1}$, dotted black line: all data for which Φ was calculated, i.e. simultaneous measurements of $NO_2$, NO, $O_3$, $J_{NO_2}$ and T were available and $J_{NO_2} \geq 6 \cdot 10^{-3}\,s^{-1}$.



ACPD
4, 2003–2036, 2004

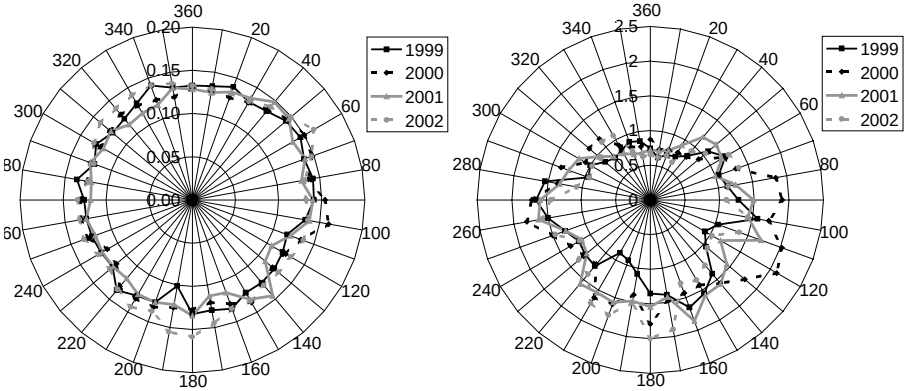


**Fig. 2.** Dependence of CO (left panel) and $NO_x$ (right panel) levels on wind direction (annual means). Only data with $J_{NO_2} \geq 6 \cdot 10^{-3}\ s^{-1}$ are considered.



ACPD

4, 2003–2036, 2004

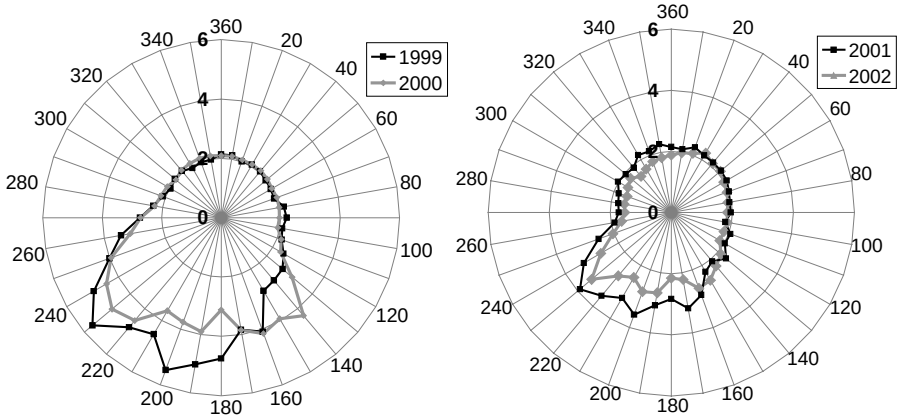


**Fig. 3.** Dependence of medians of Φ on wind direction for each year. Only data with $J_{NO_2} > 6 \cdot 10^{-3}\ s^{-1}$ are considered.



ACPD

4, 2003–2036, 2004

Assessment of the $NO\text{-}NO_2\text{-}O_3$ photostationary state applicability

K. Mannschreck et al.

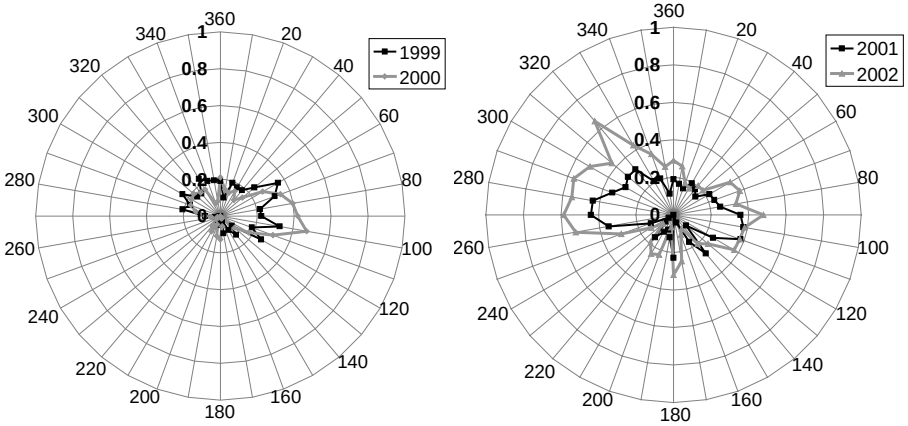


**Fig. 4.** Frequency distribution of cases (10 min means) for which PSS was established during each year. PSS was considered to be established for $\Phi_{ext}$ values between 0.8-1.2. $\Phi_{ext}$ was calculated using Eq. (8) with [XO]=0 and taking into account a $RO_2$ concentration which was determined as a function of $J_{NO_2}$ (see footnote 1). Only data with $J_{NO_2}>6{\cdot}10^{-3}\,s^{-1}$ are considered.



ACPD

4, 2003–2036, 2004

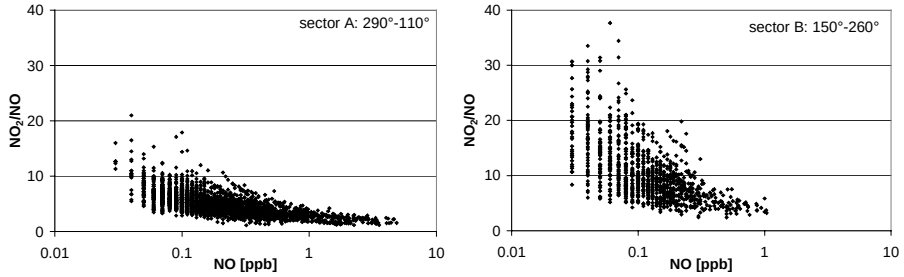


**Fig. 5.** Dependence of $NO_2$/NO ratios on the NO mixing ratio during 1999 (10 min means) for the two sectors A and B (see text).



ACPD
4, 2003–2036, 2004

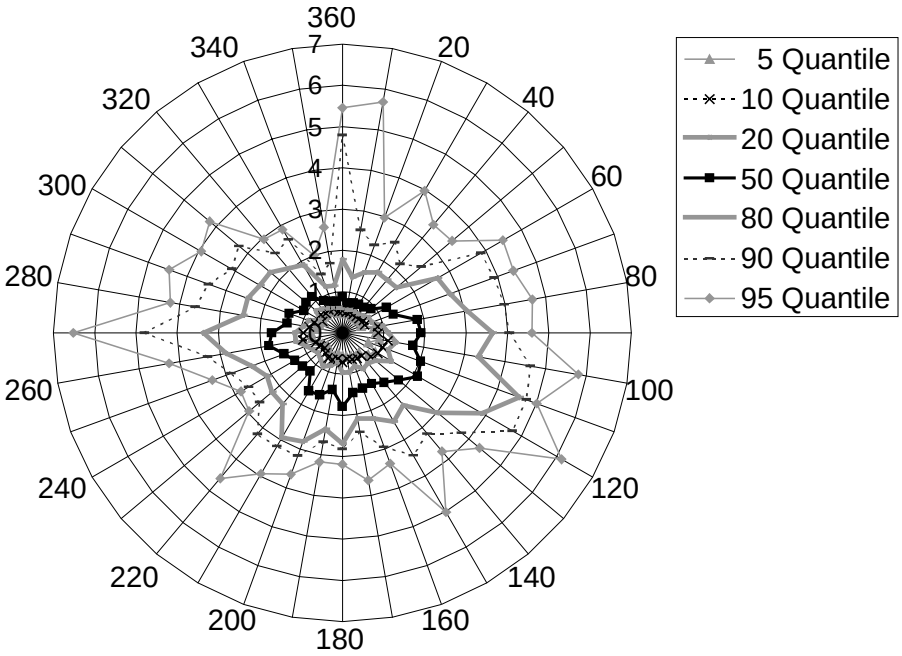


**Fig. 6.** Dependence of $NO_x$ level on wind direction for 2000. 5, 10, 20, 50, 80, 90 and 95 percentiles are shown.



ACPD

4, 2003–2036, 2004

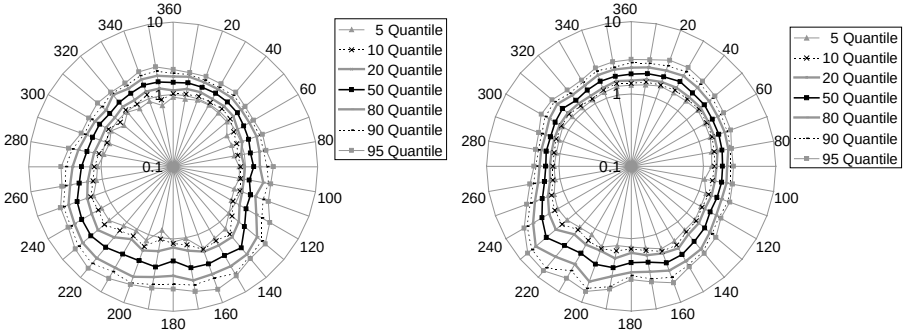


**Fig. 7.** Dependence of Φ on wind direction for 2000 (left panel) and 2002 (right panel). Φ was calculated using Eq. (5). 5, 10, 20, 50, 80, 90 and 95 percentiles are shown. The x-axis is a logarithmic scale.



ACPD
4, 2003–2036, 2004

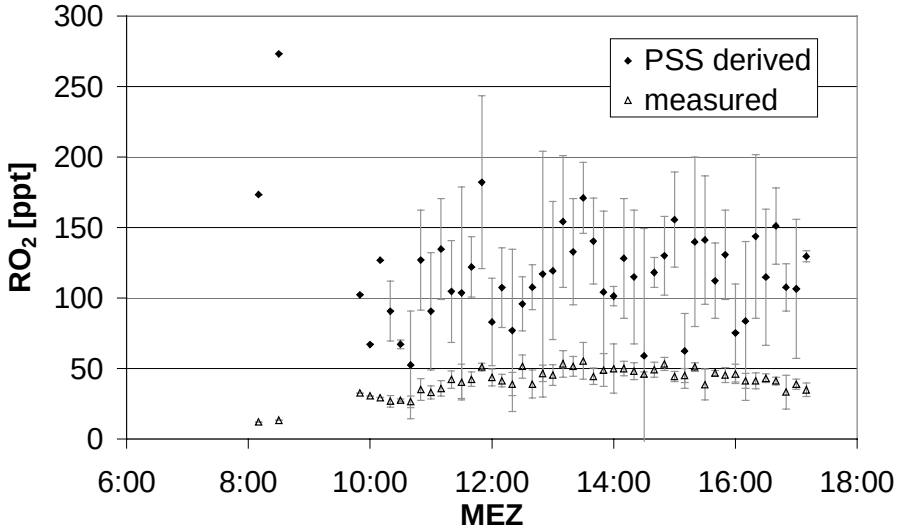


**Fig. 8.** Mean diurnal variation of measured and PSS derived $RO_2$-radicals for the sector 0°–80° the time period of 18 June–6 July 2000. Error bars refer to the 1$\sigma$-standard deviation.



ACPD

4, 2003–2036, 2004

Assessment of the $NO$-$NO_2$-$O_3$ photostationary state applicability

K. Mannschreck et al.

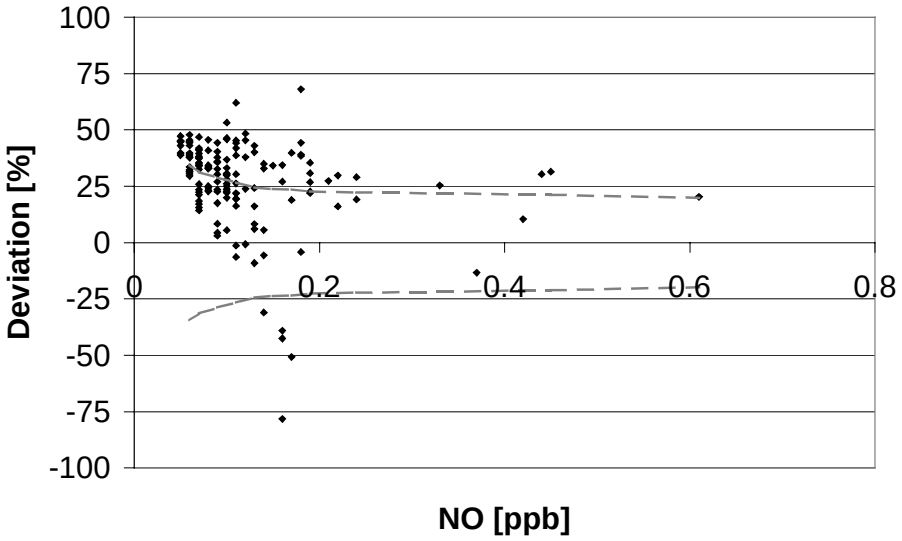


**Fig. 9.** Deviations of PSS derived $NO_2$/NO ratios from measures ones as a function of [NO] for the same time period and wind sector as in Fig. 8. The dotted line refers to the mean uncertainty of the parameter calculated for NO classes of 0.02 ppb intervals from the square root of the sum of uncertainties of measured and PSS derived ratios.



ACPD

4, 2003–2036, 2004

Assessment of the $NO$-$NO_2$-$O_3$ photostationary state applicability

K. Mannschreck et al.